Journal of Cleaner Production, Volume 333: 130201 (2022)
https://doi.org/10.1016/j.jclepro.2021.130201

A step-change toward a sustainable and chrome-free leather production: Using a Biomass-based, Aldehyde Tanning agent combined with a pioneering Terminal Aluminum Tanning Treatment (BAT-TAT)

Wei Ding [a,b], Haiteng Liu [a], Javier Remón [c], Zhicheng Jiang [d]*, Guodong Chen [a], Xiaoyan Pang [a,b]*, Zhiwen Ding [a,b]

[a] China Leather and Footwear Research Institute Co. Ltd., Beijing 100015, P. R. China

[b] Key Laboratory of Leather and Footwear Green Manufacturing Technology of China Light Industry, Beijing 100015, P. R. China

[c] Instituto de Carboquímica, CSIC, Zaragoza, 50018, Spain

[d] College of Biomass Science and Engineering, Sichuan University, Chengdu, 610065, P. R. China

*Corresponding Authors

Zhicheng Jiang, E-mail: zhichengjiang@scu.edu.cn.

Xiaoyan Pang, E-mail: pang_xiaoyan@126.com. Tel: 86-010-64337826.

Abstract

The traditional chrome-based leather industry is facing several restrictions due to potential risks to the environment, especially for the formation and release of hazardous and carcinogenic Cr (VI). However, the leather produced from alternative organic tanning agents generally does not meet the market requirements due to the poor fixation of some of the conventional anionic post-tanning materials. Herein, we report on a pioneering, Cr-free strategy to produce high-quality leather. It comprises the use of a carbon-neutral, biomass-based aldehyde (BAT) tanning agent, efficiently fixed in the leather by means of novel terminal aluminum tanning treatment (TAT). In this treatment, Al (III) bonded with the excess oxygen-containing functional groups present in the BAT, post-tanning materials and collagen fibers. As a result, these connections created a robust crosslinking network, leading to leather production with similar (and in some cases superior) properties to those produced with the conventional Cr tanning procedure. For example, the tensile and tear strengths (19.78 N/mm^2, 101.47 N/mm) were much higher than those of the Cr leather (7.13 N/mm^2 and 43.12 N/mm). Therefore, these outstanding results, along with the carbon-neutral and environmentally-friendly features of our BAT-TAT strategy, are a step-change toward chrome-free leather production, which paves the wave to ensuring the viable and sustainable development of the leather industry.

Keywords: Biomass-based aldehyde; Chrome-free leather; Eco-friendly technology; Terminal aluminum tanning treatment; Physical properties

1. Introduction

Leather products with durability and longevity have been used for centuries by human beings. They have occupied an important position in modern people's daily lives in footwear, automobile seats, clothing, bags, upholstery and fashion accessories (Jones et al., 2021). Leather is generally made by tanning the sustainable animal rawhide/skin obtained as a by-product in the meat processing industry (Joseph and Nithya, 2009). Currently, the most widely used leather tanning agents are chromic salts since they can endow leather with excellent hydrothermal stability and favorable physical properties (Ding et al., 2015; Jia et al., 2020; Pang et al., 2019). However, chrome tanning agents are facing severe restrictions due to potential risks. These hazards account for the oxidative conversion of Cr(III) to hazardous and carcinogenic Cr(VI) (Xu et al., 2021). This transformation can occur during the fabrication or storage of leather, leading to polluted tannery effluents (Selvaraj et al., 2018). These discharges, along with the improper disposal of chrome-containing solid wastes (Hedberg, 2020), are a severe barrier to the cleaner and sustainable development of the leather industry worldwide (Yu et al., 2017). Using chrome-free tanning agents to manufacture leather is a meaningful way to eliminate chrome pollution and achieve clean production in the leather industry.

In the past decades, significant efforts have been directed toward developing chrome-free tanning agents. These include inorganic and organic tanning agents. The former comprise pure aluminum salts, zirconium salts (Covington, 2009), and non-chrome metal complex tanning agents (Yu et al., 2021). The latter consist of modified glutaraldehyde, oxazolidine (Li et al., 2013), TWT/TWS (Liu et al., 2021) and polyethylene glycol triazine derivatives (Jia et al., 2021). These tanning agents come from non-renewable mineral resources (Ding et al., 2021) and petrochemicals. Besides, most of the organic tanning agents generally result in a level of formaldehyde in the leather products higher than the limits of 20 mg/kg for baby products (Y. Wang et al., 2021). From the perspectives of health, eco-friendliness and sustainability, the use of biomass-based aldehyde tanning agents (BAT), including, i.) dialdehyde sodium alginate (Ding et al., 2018b), ii.) dialdehyde tara gum (Ding et al., 2018a) and, iii.) dialdehyde carboxymethyl cellulose (Ding et al., 2019; Yi et al., 2020) is highly recommended. These species can be obtained from renewable biomass, and their application can help developing a greener and more sustainable leather industry (X. Wang et al., 2021a). The containing two active aldehyde groups (Anjali, 2012; Wang et al., 2020) in BAT can form Schiff bases with a covalent structure with the amino groups on the collagen fibers (CF) under mild alkaline conditions. These chemical transformations are paramount to the crosslinking effect needed for leather tanning (Ding et al., 2017). Given these excellent properties, BAT are regarded as promising non-hazardous organic tanning agents to achieve eco-friendly leather manufacture (Ding et al., 2020, 2018a, 2018b). Despite these good features, the isoelectric point (IEP) of BAT tanned leather was low (<5.0) (Ding et al., 2019), which hampers their fixation with conventional anionic post-tanning materials (CAPMs) (Wang and Shi, 2019). Furthermore, the Schiff base crosslinks between BAT and the collagen fibers are reversible (Ding and Wu, 2020) and easy to cleave under acid conditions. The drawbacks lead to tanned leather with low coloring intensity, fullness, mechanical strength and stretchability.

The use of amphoteric post-tanning materials may surpass these drawbacks (X. Wang et al., 2021a, 2021b). For example, Liu et al. prepared an amphoteric polymer P(AA-AM-C_{12}DM) as the retanning and fatliquoring dual-functional post-tanning material, which could benefit in enhancing the physical and mechanical properties of organic crust leather and its reactivity to anionic dye (Liu et al., 2021). Besides, Hao et al. synthesized an eco-friendly imidazole ionic liquids based amphoteric polymers for high performance fatliquoring in organic leather. This kind of fatliquoring agent could not only make leather fibers become loose, but also improve the binding affinity between leather and anionic dye during the fatliquoring process (Hao et al., 2020). However, these materials are commonly expensive. Also, considering their compatibility with CAPMs, their use may cause some unexpected alterations in the conventional leather post-tanning processing. Given this, constructing a more robust crosslinking network to fix the BAT and post-tanning materials in the leather matrix could effectively overcome these drawbacks. Aluminum (III) salts, an ancient metal tanning agent, have been used in the leather industry for centuries. Al tanned leather is soft, delicate and stretchable. Besides, the high cationic potential of Al(III) makes it helpful in enhancing the color fastness as a dye adjunct (Sreeram et al., 2006). Therefore, these features could overcome the drawbacks of BAT tanned leather if it was not for the limited shrinkage temperature and low resistance to water washing, caused by the relatively weak electrovalent bonds between Al and carboxyl groups on CF (Gao et al., 2020; Jiang et al., 2021), of the leather tanned with Al. However, it must be borne in mind that the hydroxyl-terminated dendrimers, the carboxyl-terminated hyperbranched polymers, and the glucoheptonate and gluconate have been reported to bond satisfactorily well with Al(III). As a result, the fixation intensity of Al in leather can be improved via the formation of more robust bonding networks (Covington, 2009). Apart from abundant aldehyde groups in BAT from the oxidation process of saccharides, hydroxyl groups (from incomplete oxidation) and carboxyl groups (from complete oxidation) commonly exist in BAT. Besides, conventional post-tanning materials also contain many hydroxyl and carboxyl groups. These diverse oxygen-containing functional groups are expected to improve the fixation intensity of Al in the BAT tanned leather crust, exhibiting some unexpected favorable performances.

In light of the above research and hypotheses, this work addresses for the first time a novel BAT-TAT strategy for the development of a cleaner, chrome-free and efficient leather industry. In particular, our approach comprises a new facile strategy to obtain a leather with suitable commercial properties in a more sustainable manner. This includes the use of BAT as a tanning agent, coupled with the application of a novel terminal aluminum tanning treatment (TAT) with a very low Al dosage. Firstly, the tanning performance of this new BAT-TAT strategy was thoroughly investigated. Then, the potential hazards to the environment of this methodology were assessed and compared with those of conventional chrome tanning, commercial chrome-free complex tanning (HAZ) and pure BAT tanning strategies. The assessments include comprehensive analyses of the physical properties of the resultant crust leathers, coupled with the detailed costs of the chemicals consumed. This rigorous chemical mechanistic understanding, combined with the risk and economic assessments conducted, along with the environmental friendliness, novelty and efficiency of the BAT-TAT strategy, demonstrate that this work contributes to paving the way toward a cleaner and safer leather production.

2. Materials and methods

2.1. Materials

Pickled sheepskin and conventional chrome tanned sheep leather (wet-blue) were supplied by Xinji Ling-Jue Leather Co., Ltd. (China). A commercial, chrome-free complex, tanning agent

(HAZ) that was prepared by mixing aluminum sulfate octadecahydrate, zirconium sulfate tetrahydrate, and highly oxidized starch (Yu et al., 2020), was supplied by Sichuan Tingjiang New Material, Inc. (China). A biomass-based aldehyde tanning agent with a solid content of 40 wt% (BAT, structural feature shown in Fig. S1) was prepared by periodate-oxidation of biomass at 10 ºC for 12 h according to the method described by Ding et al. (2019). Its aldehyde content was 12.0 mmol/g (based on the absolute dry weight). $Al_2(SO_4)_3•18H_2O$ (aluminum tanning agent, ATA) was of analytical grade and purchased from Sinopharm Chemical Reagent Co., Ltd. (China). Other chemicals used in the leather tanning and post-tanning processes were of commercial grade.

2.2. Methods

2.2.1. Preparation of chrome-free leather

Pickled sheepskins were treated according to the procedures shown in Table S1 and Table S2 to prepare the HAZ chrome-free leather and BAT chrome-free leather, respectively.

2.2.2. Post-tanning

The as-prepared wet-whites and conventional wet-blue were subjected to a post-tanning process whose procedure is summarized in Table S3. After fat liquoring, the wet whites were naturally dried and softened to prepare the crust leather. Then, the crust leathers were further sampled for the evaluation of physical properties. A part of the fat liquored BAT wet white was sampled for further tanning using a reduced dosage of ATA to enhance its comprehensive performance.

2.2.3. Terminal aluminum tanning treatment (TAT) trials

The TAT process of the fat liquored BAT tanned leather was performed in a drum with 100% water (based on the weight of shaved wet-white, the same below) and 0.50% of the ATA (calculated by Al_2O_3) at 25 °C. After running for 3 h, the pH of tanning liquor was slowly raised to 4.2 by adding sodium bicarbonate. Then, the temperature was increased to 40 °C. The aim of increasing the float pH and temperature was to promote the crosslinking and fixation between the ATA and the collagen fibers. After continuously running for 4 h, the BAT-TAT leather was washed for 5 min using water at room temperature, followed by natural drying and softening to prepare the resultant crust leather.

2.2.4. Assessment of wastewater

Wastewaters from the retaining-dyeing and fatliquoring processes were collected to determine the Total Organic Carbon (TOC) (Vario TOC, Elementar, Germany). TOC discharge load was calculated accordingly and expressed as grams per ton of tanned leather. The metal content (Cr, Zr, Al) concentration of wastewater was determined using ICP-OES (Varian 710-ES, VARIAN, USA) according to the method described by Ding et al. (2015). The metal content of the effluent was calculated and expressed as grams per kilogram of tanned leather.

2.3. Characterization

2.3.1. Interaction analysis

The BAT crust leather and BAT-TAT crust leather were analyzed by FTIR spectroscopy (Tensor 27, Bruker, Germany) equipped with an attenuated total reflectance accessory. Each FTIR spectrum was recorded at a wavenumber ranging from 4000 cm^{-1} to 600 cm^{-1} with a resolution of 4 cm^{-1}. Changes in the chemical and electronic states of the samples were detected by XPS (K-alpha Plus, Thermo Fisher Scientific, USA). Besides, the thermal stability of the BAT and BAT-TAT crust leathers were measured using a TG-DSC thermal analyzer (STA-8000, PerkinElmer, USA) under nitrogen atmosphere. An alumina crucible was used to encapsulate leather sample and the temperature was ramped from 30 to 800 °C at a heating rate of 10 °C/min.

2.3.2. Shrinkage temperature test

Shrinkage temperature (Ts) is the most common index to characterize the hydrothermal stability of leather, and it is an effective index that can reflect the fixation and dispersion of collagen fibers (Cohen et al., 2000). The Ts of the leather samples were tested by a digital leather Ts instrument (MSW-YD4, Sunshine Electronic Research Institute of Shaanxi University of Science and Technology, Xi'an, China).

2.3.3. Morphology observation and pore structure analysis

Leather samples were collected and lyophilized using a freeze dryer (LC-12N, LICEN-BX, China). Then, the cross-sections of these samples were observed by field emission scanning electron microscopy (FESEM, S4800, HITACHI, Japan) with an accelerating voltage of 5.0 kV, and the Al distribution on the cross-section was detected through EDS (EDAX, AMETEK, USA). The pore structure of the crust leather sample was measured using a mercury intrusion porosimeter (MIP, AutoPore V 9600, Micromeritics, USA).

2.3.4. Physical properties analyses

The crust leather samples were firstly air-conditioned at 20 °C and 65% relative humidity for 48 h according to the standard method (IUP 3), and then they were sampled to determine the physical properties. The mechanical strengths and elongations were tested using a tensile tester (AI-7000SN, Gotech, China) according to the standard methods (IUP 6 and IUP 8) (IUP 6, 2000; IUP 8, 2000). The softness of the crust leather was tested using a standard leather softness tester (GT-303, Gotech Testing Machines Inc., China) designed based on IUP 36 (IUP 36, 2000). Its reading range was from 0.1 mm to 10 mm. The data in this section were measured three times and presented as the mean ± standard deviation. The fullness of crust leather was evaluated by compression-resilience performance using the method described by Peng et al. (2006). The grain surface of the crust leather was observed using a stereoscopic microscope (M205 C, Leica, Germany), and the statistical analysis of grain width (100 data points) was carried out using Nano measurer software (version 1.2.5). The apparent density of the crust leather was measured according to the ISO 2420:2017 method (ISO 2420:2017, n.d.).

The coloring performance of crust leather was evaluated according to the method described by Ding et al. (2019). Firstly, the color measurement parameters (L, a, b) from 8 random points on the crust leathers were recorded using a color measurement instrument (SC-80C, Jingyi Kangguang, China). The total color difference (ΔE) was calculated by Equation 1:

$$\Delta E=\sqrt{(\Delta L)^2+(\Delta a)^2+(\Delta b)^2} \quad (1)$$

where ΔE represents the overall color difference; ΔL is the lightness difference; Δa and Δb stand for the difference between a and b values, where 'a' represents red and green axis and 'b' represents yellow and blue axis. Δ L, Δa and Δb were calculated by subtracting the corresponding values from one given sampling point. After this, the ΔE of the other 7 points on the crust leather were obtained. Next, the standard deviation (STDEV) value of 7 ΔE values was calculated to evaluate the dyeing uniformity. The lower the STDEV is, the higher the dyeing uniformity (Ding et al., 2019). Besides, the dry and wet rubbing fastness of the crust leather was evaluated according to standard methods (ISO 11640:2018) (ISO 11640:2012, n.d.). The given load was set to be 500 g, and the number of forward-backward motions was 50.

2.4. Optimization analysis

A radar chart array analysis performed the optimization analysis of different processing strategies for leather manufacture. This evaluation selected six key indicators: hydrothermal stability, mechanical strength, organoleptic property, coloring performance, environmental friendliness and economy. The total score for each indicator was set as 10, and the detailed scoring rule is shown in Table S4. Based on this analysis, the comprehensive performance could be visually displayed using an optimal score-radar map.

3. Results and discussion

3.1. Strengthened fixation intensity

Generally, the thermal stability of leather is positively correlated to the crosslinking intensity (Cohen et al., 2000; Ding et al., 2017). Fig.1a illustrates that the TAT could improve the Ts of the Biomass Aldehyde Tanned leather (BAT leather), which was in accordance with the improved thermal denaturation temperature of the Biomass Aldehyde Tanned-TAT leather (BAT-TAT leather) (Fig. 1b) compared with the BAT leather. The thermal stability of the crust leather was further evaluated by thermogravimetric analysis (Fig. 1c, d). It can be noted that the onset slight weight loss of about 5 wt% ($T_{5\%}$) appeared at 196 °C for the BAT leather, while this appeared at 204 °C for the BAT-TAT leather. It can be seen from the results that the major weight loss appeared at 67 °C for the BAT leather in the region from room temperature to 120 °C, while this appeared at 75 °C for the BAT-TAT leather. This might be due to the evaporation of absorbed and bound water in the leather (Liu et al., 2019). Moreover, the primary decomposition temperature of the BAT-TAT leather (329 °C) was higher than that of the BAT leather (322 °C). These results were highly consistent with the Ts variation of the leather described above and demonstrate that the thermal stability of the BAT leather was improved after the TAT. Bai et al reported that the residual methylol group in melamine-formaldehyde resin could react with the amino or hydroxyl residues in the leather collagen fibers, promoting crosslinks between the collagen chains. These transformations confer higher thermal stability to the leather (Bai et al., 2013). These results seem to indicate that a more intensive collagen fiber network had been constructed for the BAT leather based on the TAT.

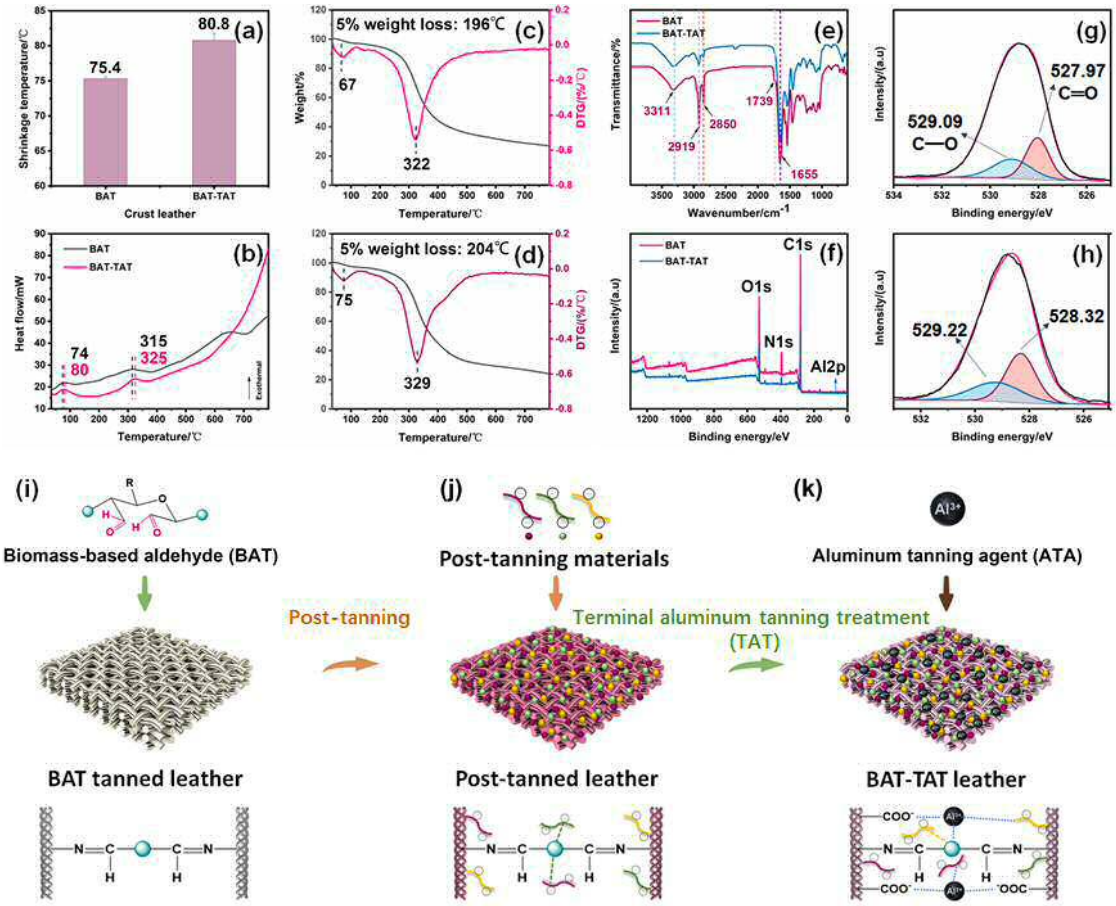

Fig. 1. Thermal and structural properties of crust leather: (a) Ts of crust leather; (b) DSC curves of crust leathers; (c) TG curve of BAT crust leather; (d) TG curve of BAT-TAT crust leather; (e) FT-IR spectra of crust leather; (f-h) XPS curves of crust leather; and the proposed strengthening process of TAT for BAT crust leather (i-k).

During the BAT-TAT processing, the BAT was firstly loaded on the leather crust via the formation of Schiff bases between the aldehyde groups in the BAT, which positively charged the amino groups in the collagen fibers (Fig. 1i). After that, the introduction of traditional post-tanning materials in the post-tanning process, including acrylic resin, amino resin, mimosa and fatliquor, can in turn bind with the collagen fibers and the residues of the BAT in a nonspecific manner (Fig. 1j). In this situation, the surface and interior of the BAT leather were covered and filled with many anionic materials, providing abundant oxygen-containing binding sites for Al(III). As described above, the diverse oxygen-containing functional groups on the BAT leather are supposed to be combined with Al(III) to construct a more robust crosslinking network. Such formation is also accompanied by the change in the binding state of oxygen-containing functional groups. FTIR and XPS analysis were adopted to reveal this, and the related results are presented in Fig. 1(e-h). It can be noted that the two kinds of leather presented a similar spectrum. However, after the TAT, the peak at 1739 cm^{-1} assigned to the stretching vibration of C=O from carboxyl and aldehyde groups disappeared, suggesting their involvements in the complexation with Al(III). The XPS spectrum of the BAT-TAT leather was compared with that of the BAT leather. Such a comparison was intended to identify the complexation between Al(III) and the carboxyl groups of the BAT leather during the TAT. As shown in Fig. 1f, the significant peaks attributed to O1s and C1s were reduced in the XPS spectrum of the BAT-TAT leather, and a new weak Al2p peak appeared (Fig. S2). This was due to the release of a small number of post-tanning materials from the BAT leather and the fixation of Al(III) on the BAT leather during the TAT. Fig. 1g shows that the high-resolution XPS spectrum of O1s in BAT leather could be fitted with two components located at 527.97 eV and 529.09 eV, corresponding to C=O and C–O species, respectively. For the high-resolution XPS spectrum of TAT-BAT leather, the O1s peak showed a slight shift to 528.32 eV and 529.22 eV (Fig. 1h), which demonstrated that the carboxyl groups in the BAT leather were blocked by Al(III) (Tang et al., 2020). In light of the above results, it is suggested that additional crosslinks arose from the formation of an interlocking network among the post-tanning materials. These connections take place between the residues of the BAT and the carboxyl groups of the collagen fibers, with Al(III) species serving as crosslinking bridges (Fig. 1k). As a result, a more robust crosslinking collagen fiber network was successfully constructed for the BAT-TAT, improving the physical and organoleptic properties of the resultant leather.

3.2. Physical properties

3.2.1. Collagen fiber dispersion

A higher crosslinking intensity generally endows the leather with better collagen fiber dispersion, leading to more favorable organoleptic properties of the crust leather (He et al., 2021, 2020). The fiber dispersion of different crust leathers was analyzed using FESEM. As shown in Fig. 2, the fiber dispersion degree of the conventional chrome-tanned, resultant leather (Cr leather) was the highest, followed by the commercial chrome-free complex tanning agent tanned resultant leather (HAZ leather). The collagen fibers of BAT leather were woven randomly and adhesively. In contrast, our BAT-TAT leather had well-dispersed collagen fiber bundles due to the uniform distribution and fixation of Al in the collagen matrix (Fig. 2f). These bundles were comparable to those of the HAZ leather, benefiting the improvement of the physical properties of the BAT leather. Moreover, the hierarchical pore structure of leather can be characterized by MIP, which is a meaningful aid to explore the relationship between the crosslinking intensity and the fiber dispersion of leather (He et al., 2019). Fig. 3 presents the pore size distribution of four typical crust pieces of leather measured by MIP. As expected, the Cr leather presented the highest proportion (12.82%) of relatively small pores in the range of 5.48 to 1000 nm due to the excellent tanning effect of the chrome tanning agent, which suggested that more pores were present on the microfibrils/fibrils level. This result was similar to that reported by He et al (He et al., 2020). The HAZ leather showed the second-highest proportion (7.78%) of relatively small pores in the range of 5.48 to 1000 nm owing to the favorable tanning effect of HAZ. In comparison, this proportion in the BAT leather was only 4.93% because of the relatively weaker tanning effect of BAT. These results presented a similar variation tendency to that reported by He et al (He et al., 2019). However, owing to the other interlocking effect caused by Al(III), this value was improved to 6.40% after undergoing the TAT. These results are in agreement with the collagen fiber dispersion of different crust leathers. This suggested that the crosslinking intensity of BAT leather had been strengthened after the TAT and opens the door to developing a Cr-free and cleaner leather industry.

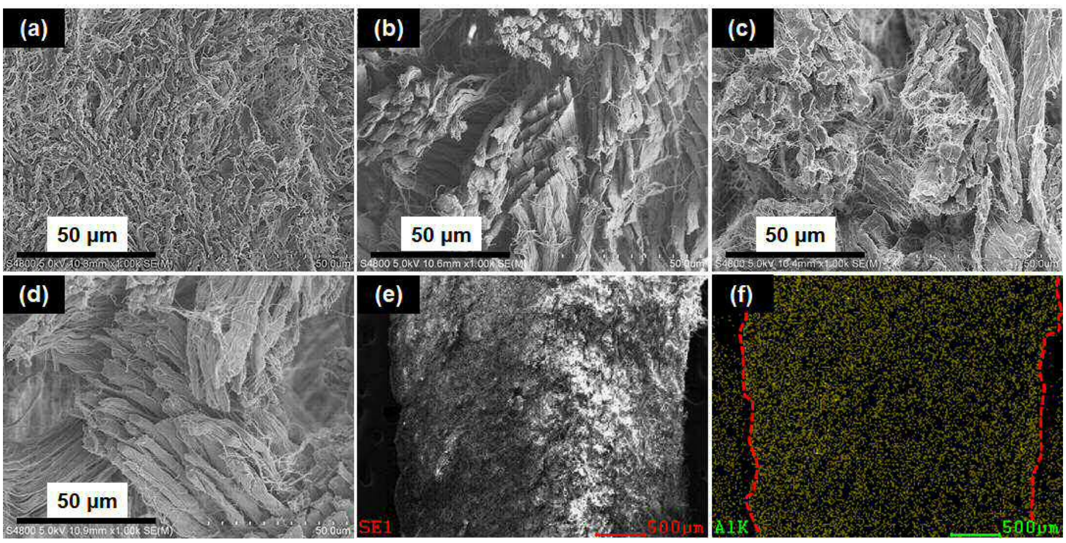

Fig. 2. FESEM images of the cross-section of crust leathers from different processing strategies: (a) Cr; (b) HAZ; (c) BAT; (d) BAT-TAT; (e) cross-section of BAT-TAT crust leather; (f) EDS Al elemental mapping image of the cross-section of BAT-TAT crust leather.

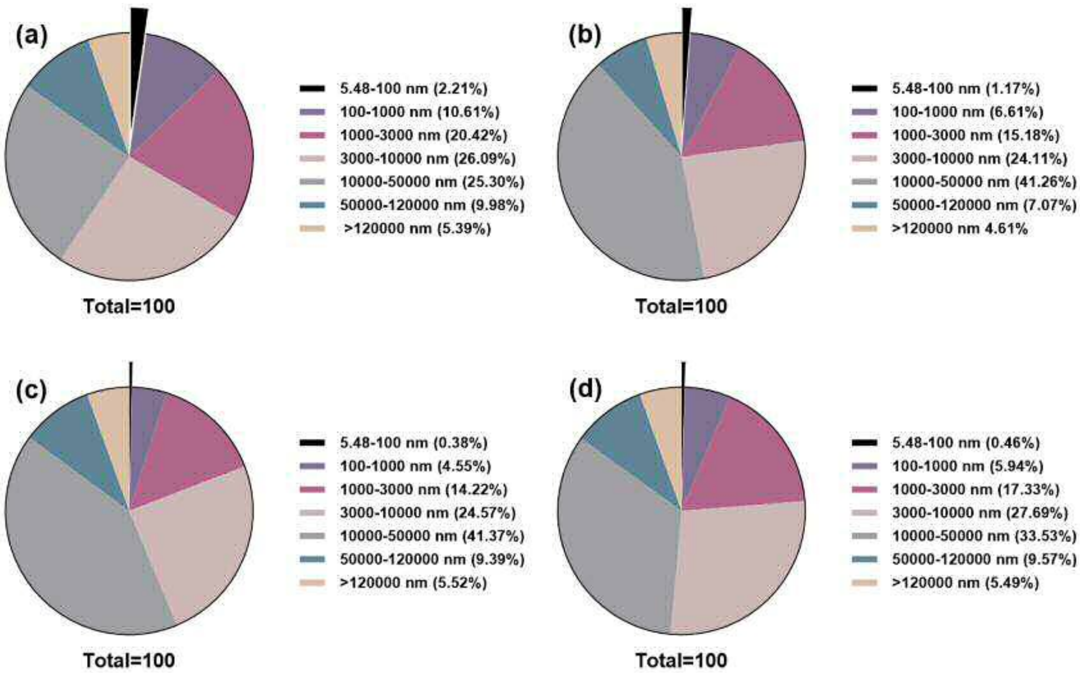

Fig. 3. Pore size distribution of crust leathers from different processing strategies: (a) Cr; (b) HAZ; (c) BAT; (d) BAT-TAT.

3.2.2. Physical properties

The smoothness of the leather grain surface is one the best approaches to assess the organoleptic properties of crust leather, and it was determined using a stereomicroscope. As shown in Fig. 4, there was no physical deposition for each crust leather, which was evident from a clear grain surface obtained in the crust leather. For this material, the pores were clear and clean without any impurity in all cases. The grain surface of the Cr, HAZ and BAT-TAT leathers seemed to be stereoscopic. In comparison, the grain surface of the BAT leather was over-flat. However, the statistics of the grain width of the different crust leathers show that the HAZ leather had the widest grain (0.86 mm), followed by the Cr leather (0.72 mm), with the BAT leather showing the lowest grain width (0.44 mm). After the TAT, the grain width of the BAT crust leather slightly increased up to 0.47 mm. This suggests that the grain surface of the HAZ leather was the roughest, followed by the Cr leather. In comparison, the grain surface of the BAT crust leather was the smoothest, and the grain surface of the BAT-TAT crust leather was also considerably smooth. These measurements reveal that the TAT improves the over-flat grain surface of the BAT leather without significantly increasing the roughness of the grain surface. This indicates that Al(III) performed a moderate crosslinking effect on the grain surface of the BAT leather. This is accounted for by its efficient penetration into the interior of the BAT leather to construct a more robust collagen fiber crosslinking network.

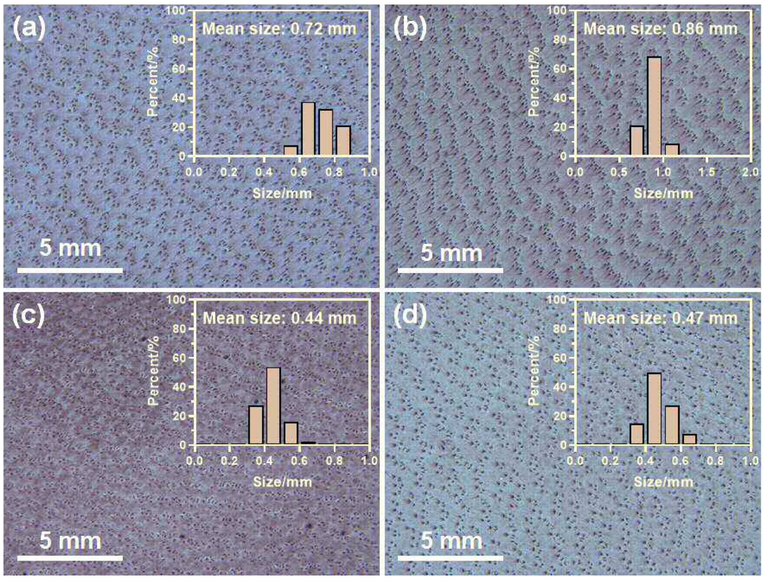

Fig. 4. Grain surface and width of the crust leathers from different processing strategies: (a) Cr; (b) HAZ; (c) BAT; (d) BAT-TAT.

Dyeing uniformity and coloring fastness are two other important indicators to evaluate the performance of crust leather. Fig. 5 illustrates the dyeing uniformity and resistance to dry-wet rubbing. As described in section 2.3.4, the lower the STDEV value of the total color difference (ΔE), the higher is the dyeing uniformity (Ding et al., 2019). Among the four types of leathers, the Cr leather had the lowest STDEV value of ΔE, indicating its best dyeing uniformity. The HAZ leather had the second-highest STDEV value of ΔE, showing moderate dyeing uniformity. Unfortunately, the BAT leather had the highest STDEV value of ΔE, suggesting its lowest dyeing uniformity. However, its dyeing uniformity was significantly improved after the TAT, given the comparable and low STDEV value of ΔE to Cr leather, indicating the favorable dyeing uniformity of the BAT-TAT leather. This represents a step-change to replace Cr in the leather industry with a more sustainable and renewable alternative. Fig. 5(b,c) presents the resistance of crust leather to dry-wet rubbing under a more rigorous test condition than the typical test condition. All four types of crust leathers had desirable resistance to dry-rubbing with the highest level. As expected, the Cr leather showed the relatively best resistance to wet-rubbing due to the excellent bonding between the Cr tanned leather and anionic dyes. On the contrary, the BAT leather showed the lowest resistance to wet-rubbing, followed by the HAZ leather. Very interestingly, after the TAT, the resistance of the BAT leather to wet-rubbing substantially improved, and it was close to that of the Cr leather. This gives another indicator that a chrome-free leather industry is possible using biomass resources appropriately.

As commented earlier, the binding intensity between the BAT tanned leather with a low IEP and anionic dyes was relatively weak, which could result in unsatisfactory dyeing uniformity and colorfastness. In our previous work, an amino-terminated waterborne polyurethane-based polymeric dye (AWPUD) was synthesized to achieve high-performance dyeing with BAT tanned leather (Ding et al., 2021). This work proposes a similar strategy to improve the color fastness via constructing a more robust combination between the dyestuff and the leather matrix. The as-synthesized AWPUD could endow the BAT crust leather with better dyeing performances and higher thermal stability than the conventional dyed crust leather. This results from the more robust crosslinking network between the dyes and CFs supplied by the terminal amino group of AWPUD. Therefore, the binding intensity could be strengthened after the TAT, with Al(III) playing the crosslinking bridge role. As a result, the dyeing uniformity and colorfastness of the BAT leather were successfully improved.

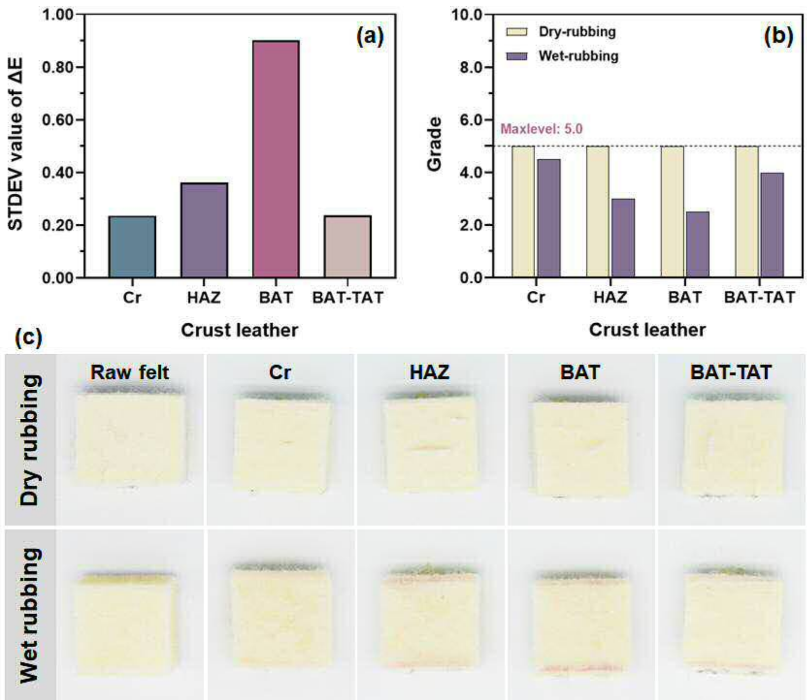

Fig. 5. Images of felt before and after dry and wet rubbing: comparison of crust leathers from different processing strategies.

In addition to the above organoleptic properties, the softness, apparent density and fullness of crust leather were evaluated to assess the collagen fiber dispersion. It is observed that the Cr leather, with the highest collagen fiber dispersion degree, exhibited the highest softness. In comparison, the HAZ, BAT and BAT-TAT leathers, with lower collagen fiber dispersion degrees, had lower softness (Fig. 6a). Compared with the HAZ leather, the BAT and BAT-TAT leathers had a slightly higher softness, which might be caused by the compact-crosslinking effect of HAZ in the collagen fibers. The apparent density is an important indicator to assess the lightness of leather. For this variable, the lower the apparent density is, the better the feeling of material lightness. Generally, the apparent density is dominated by the dehydration effect and addition amount of tanning agent, and a better dehydration effect will result in higher collagen fiber dispersion (He et al., 2021). As illustrated in Fig. 6b, the Cr leather had the lowest apparent density, providing this material with the best feeling of lightness. This was due to the favorable dehydration effect of the Cr tanning agent, accompanied by a desirable collagen fiber dispersion (He et al., 2021). In comparison, the HAZ leather had the highest apparent density, presenting a feeling of heaviness. This might be attributed to the relatively weaker dehydration effect of HAZ accompanied by fairly low collagen fiber dispersion, along with the greater amount of tanning agent used. Similarly, the apparent density of the BAT leather was higher than that of Cr leather owing to the weaker dehydration effect of the BAT and collagen fiber dispersion. Compared with the BAT leather, although the collagen fiber dispersion was improved, the apparent density of leather slightly increased after the TAT because of the introduction of Al species. Nevertheless, it was still lower than that of the HAZ leather due to the lesser amount of tanning agent used. Overall, the BAT and BAT-TAT leathers performed better in the lightness test than the HAZ leather, which was close to the lightness feeling of Cr leather and provided shreds of evidence of the effectiveness of our methodology to achieve a Cr-free leather manufacturing.

Fig. 6(c, d) presents the compression-resilience performance of crust leather, such a property strongly affected by the collagen fiber dispersion. This test reveals that the Cr leather, having the highest collagen fiber dispersion degree, exhibited the highest compressed and resilient thickness. In contrast, the BAT leather, with the lowest collagen fiber dispersion degree, showed the lowest compressed and resilient thickness. After the TAT, the compressed and resilient thicknesses of BAT leather were significantly improved. These values were now comparable to those of the HAZ leather and close to those of the Cr leather, which proves evidence of the commercial applicability of our strategy. Generally, higher compressed and resilient thicknesses represent better fullness of crust leather (Ding et al., 2018b). It can be then concluded that the Cr leather had the beset fullness, followed by the HAZ leather. The fullness of the BAT leather was significantly improved up to a value comparable to that of the HAZ leather after the TAT. During the TAT, in addition to bonding with the residual oxygen-containing groups in the BAT and collagen fibers, Al(III) can also bond with the oxygen-containing groups of the post-tanning materials. As a result, these connections create a robust interlocking network among the collagen fibers and the BAT and post-tanning materials. These results show that post-tanning materials exert a positive effect in the BAT-TAT to create a strong collagen fiber network (Ding et al., 2018b). As a result, the dispersion of the collagen fiber network is substantially improved, and the BAT-TAT leather exhibited comparable fullness to that of the Cr leather, which is a substantial step-change to tanning leather in the absence of Cr.

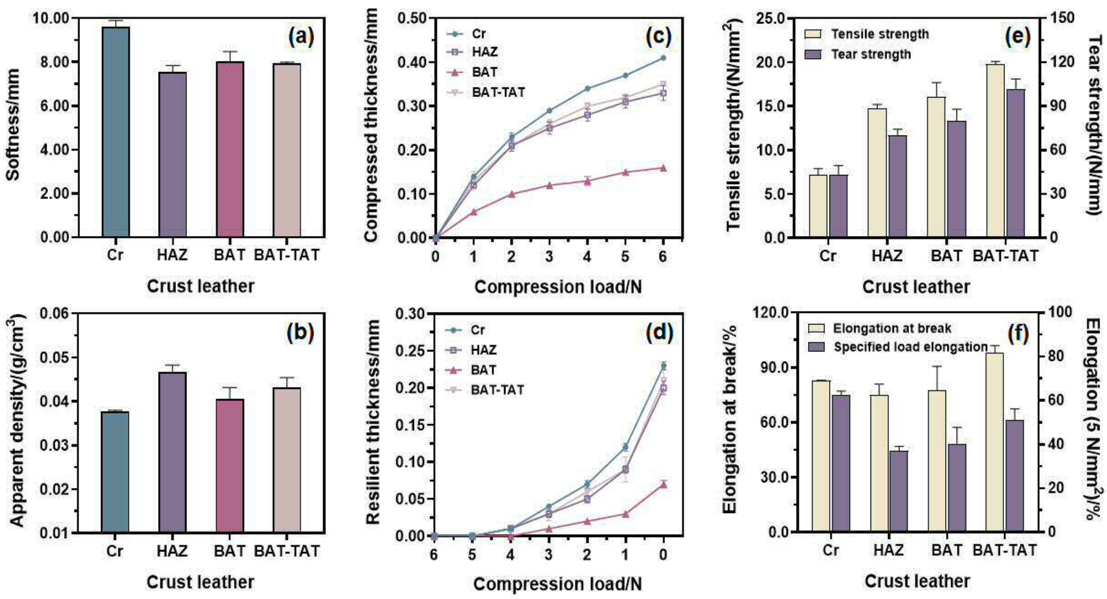

Fig. 6. Organoleptic properties and mechanical strengths of the crust leathers from different processing strategies.

Mechanical strength is one of the most fundamental properties for the commercialization of leather. The tensile strength, tear strength and elongation of the BAT-TAT leather were further determined and compared with those of the Cr leather, HAZ leather and BAT leather. As illustrated in Fig. 6 e, all the chrome-free tanned resultant leathers had higher tensile and tear strengths than the Cr leather. Among them, the BAT-TAT leather had the highest strengths, which is a significant achievement in this field and highlights the excellent applicability of biomass-based species in the leather industry. Fig. 6 f shows that the Cr leather had a desirable elongation and the most favorable stretchability (the highest elongation with a specified load of 5 N/mm^2). Among the three kinds of chrome-free tanned resultant leathers, the BAT-TAT leather had the highest elongation and stretchability, which were comparable to those of Cr leather. This indicated that the TAT could also improve the mechanical strengths of the pristine BAT leather.

In general, the tensile strength of leather is dominated by the weaving and dispersion of the collagen fibers, while the tear strength is mainly affected by the strength of the grain, the hardness, flexibility, compactness, and evenness of the fibers (Ma et al., 2021, 2002). The stretchability mainly depends on the lubricity of the collagen fibers. For the Cr and HAZ leathers, although their fiber dispersion degree was relatively high, most of the crosslinks were rigid and compact, owing to the small molecular size of the tanning agent. The excessive binding of Cr or HAZ species with the collagen fibers may have caused an increase in collagen fiber brittleness, leading to relatively low tensile and tear strength. In comparison, the crosslinks existing in the BAT leather were less rigid because of the flexible molecular chain of the species present in the BAT. As a result, the BAT leather had higher tensile and tear strengths. After the TAT, more post-tanning materials were fixed in the leather matrix via the additional crosslinks provided by Al(III) species. Simultaneously, the collagen fibers were well-dispersed and regularly weaved, thus improving the tensile and tear strengths of the BAT leather. Owing to the formation of a rigid-flexible crosslinking network and the increase in the collagen fiber lubricity, the stretchability of the BAT-TAT leather was also significantly improved.

The results point out that the TAT endows the BAT crust leather with a more robust crosslinking network via forming a multi-point rigid-flexible interlocking structure. This enhancement improves the dispersion and weaving regularity of collagen fibers and the organoleptic properties and mechanical strengths of the BAT leather. As a result of the high performance shown by the BAT-TAT leather, this green procedure has favorable prospects for commercial applications.

3.3. Pollution load comparison

After having analyzed and compared some critical properties of the leathers produced with the different tanning agents, this section addressed the possible positive or negative impacts of the tanning process. For the post-tanning process, the total organic carbon (TOC) and metallic contents are paramount parameters to assess the possible hazards related to the spent post-tanning wastewater. Table 1 shows that the amount of metals present in the post-tanning effluents from Cr and HAZ processes were higher than those resulting from the BAT-TAT process. This difference accounts for a severe release of metals from leather during the high-temperature fatliquoring process. This increases pollution as the wastewater produced is difficult to treat due to the complexation between the residual CAPMs and metal ions (Tang et al., 2020). After TAT, the wastewater also contained a small concentration of metals due to the incomplete absorption of Al. However, its uptake ratio was up to 99.83%, and only a tiny amount of metals remained in wastewater. Therefore, this new BAT-TAT shows a substantial improvement to the typical leather industry based on Cr from an environmental perspective.

Table 1. Comparison of metallic element load from different post-tanning processing schemes.

Process	**Metallic element load/(g/t of tanned leather)**			
	Cr	**HAZ**	**BAT**	**BAT-AL**
Retanning	29.24 ± 0.21	18.25 ± 0.05	-	-
Fatliquoring	116.86 ± 0.63	99.55 ± 0.55	-	-
Terminal tanning	-	-	-	100.87 ± 0.02
Total load	146.10 ± 0.40	117.80 ± 0.60	-	100.87 ± 0.02
Metallic element	Cr	Al and Zr	-	Al

- Not detected.

Table 2 shows that the BAT process releases wastewater with a higher TOC than the Cr and HAZ processes produced. This is a normal phenomenon due to the organic nature of the BAT in comparison to the inorganic character of the Cr-based tanning. Compared with the BAT processing scheme, the additional TAT only led to a slight increase in the TOC of the effluent, owing to the slight release of post-tanning materials from the BAT leather. However, it is worth noting that the organic pollutants in the BAT processing system can be easily removed by advanced oxidation technologies (Korpe et al., 2019; Sivagami et al., 2018), thus still representing and advance over the treatment of the effluent produced with Cr. Besides, the wastewater from the TAT had lower metal content and TOC than that from Cr or HAZ processes, showing much higher cleanability and treatability. Accordingly, these small amounts of organic pollutants and metal ions from the TAT would not pose pressure and challenges to leather processing, in contrast to the environmentally more controversial nature of the effluents produced with the traditional Cr-based tanning industry. Therefore, the implementation of our BAT-TAT represents a significant milestone in leather processing towards a more sustainable, carbon-neutral Cr-free leather industry.

Table 2. Comparison of TOC load from different processing schemes.

Process	**TOC load/(kg/t of tanned leather)**			
	Cr	**HAZ**	**BAT**	**BAT-AL**
Retanning	4.63 ± 0.00	4.62 ± 0.00	5.47 ± 0.00	5.47 ± 0.00
Fatliquoring	4.89 ± 0.01	4.51 ± 0.01	5.84 ± 0.00	5.84 ± 0.00
Terminal tanning	-	-	-	2.00 ± 0.00
Total load	9.53 ± 0.00	9.13 ± 0.01	11.31 ± 0.00	13.31 ± 0.00

- Not detected.

3.4. Economic analysis

The marketable implementation of a new process generally requires commercial possibility and cost-efficacy (Krishnamoorthy et al., 2013). In addition to environmental impacts, the new process must be sustainable and economically viable. The total chemical costs for processing 1 t of limed sheep pelt through the conventional chrome, commercial HAZ, as well as the experimental BAT and BAT-TAT tanning and post-tanning processing schemes are given in Table 3.

Table 3. The cost of main chemicals used for leather tanning and post-tanning.

<table>
<tr><th>Processing strategy</th><th colspan="2">Chrome tanning</th><th colspan="2">HAZ tanning</th><th colspan="2">BAT-TAT</th></tr>
<tr><td>Tanning process</td><td>Offer/kg</td><td>Cost/$</td><td>Offer /kg</td><td>Cost/$</td><td>Offer /kg</td><td>Cost/$</td></tr>
<tr><td>Tanning agent</td><td>80</td><td>80</td><td>100</td><td>150</td><td>20</td><td>60</td></tr>
<tr><td>Post-tanning process</td><td colspan="3">Offer/kg</td><td colspan="3">Cost/$</td></tr>
<tr><td>Acrylic resin</td><td colspan="3">7.5</td><td colspan="3">14.0</td></tr>
<tr><td>Amino resin</td><td colspan="3">5.0</td><td colspan="3">3.2</td></tr>
<tr><td>Dyestuff</td><td colspan="3">5.0</td><td colspan="3">38.5</td></tr>
<tr><td>Mimosa</td><td colspan="3">10.0</td><td colspan="3">23.0</td></tr>
<tr><td>Fatliquor</td><td colspan="3">20.0</td><td colspan="3">64.0</td></tr>
<tr><td>TAT</td><td>Offer/kg</td><td>Cost/$</td><td>Offer/kg</td><td>Cost/$</td><td>Offer/kg</td><td>Cost/$</td></tr>
<tr><td>Al tanning agent</td><td>0</td><td>0</td><td>0</td><td>0</td><td>16.3</td><td>2.5</td></tr>
<tr><td>Total cost/$</td><td colspan="2">222.7</td><td colspan="2">292.7</td><td colspan="2">205.2</td></tr>
</table>

The experimental BAT and BAT-TAT processes exhibited much lower chemical costs as compared to the conventional chrome and commercial HAZ processes. Based on the price data of related raw materials provided by Alibaba and the product price provided by the supplier, the total chemical cost of the conventional chrome and commercial HAZ processing schemes were about US$ 222.7 and US$ 292.7, respectively. In contrast, the experimental BAT and BAT-TAT processing schemes were about US$ 202.7 and US$ 205.2, respectively. Compared with the conventional chrome processing scheme, the possible decrease in chemical cost was about US$ 17.5 for processing 1 t of limed sheep pelt when the BAT-TAT processing scheme was used. The tanned leathers were converted into crust leather using the same post-tanning chemicals and offers. A much lesser tanning agent dosage accounted for the difference in the total chemical costs in the BAT than those used in the chrome tanning and HZA tanning processes. These results indicate that the BAT-TAT processing scheme has acceptable economic viability. Additionally,, it should be pointed out that the adoption of this new chrome-free processing scheme does not require extra expenditure. Consequently, this strategy leads to a viable, greener option to the conventional intricate processing.

3.5. Comprehensive performance comparison

A comprehensive performance comparison for the four leather processing strategies was conducted via radar chart array analysis. The key indicators considered were hydrothermal stability, mechanical strength, organoleptic property, coloring performance, environmental friendliness and economy. As illustrated in Fig. 7, each kind of crust leather had its unique advantages except the HAZ leather. As expected, the Cr leather performed the most favorable hydrothermal stability and organoleptic properties due to the excellent tanning effect of the chrome tanning agent, despite the environmental hazards associated. Owing to the metal-free feature of the BAT tanning, the BAT leather exhibited the most environmental friendliness, followed by the BAT-TAT and HAZ leathers. As for the BAT-TAT leather, its most remarkable feature was its highest mechanical strength, and its organoleptic properties, with the coloring performance being similar to that of the Cr leather. Besides, the cost-efficacy of the BAT-TAT was comparable to that of the BAT leather, which was better than that of the Cr and HAZ leathers. In general, the larger the closed-loop area of each property of a crust leather is, the better its overall performance (Meng et al., 2017; Meng and Khayat, 2017). According to this, the BAT-TAT leather showed comparable overall performance to Cr leather, which was significantly better than BAT leather or commercial HAZ leather. This similar overall performance is definitively a major achievement to produce tanned leather efficiently in a sustainable and environmentally friendly manner.

During the BAT-TAT, the BAT is prepared from renewable resources, and the use of Al does not bring evident pressure on aluminum resource consumption due to its very low dosage. The as-reported BAT-TAT processing strategy can provide a cleaner and economical option for boosting the eco-friendly development of the leather industry. Nevertheless, to realize the actual industrial application of this engineering technology is still needed to reduce the industrial production cost of the BAT, optimize its production process and control its quality. On the bright side, it is believed that with the ability to mass-produce high-quality and cost-effective BAT, the industrial applications for BAT-TAT technology will be extensive.

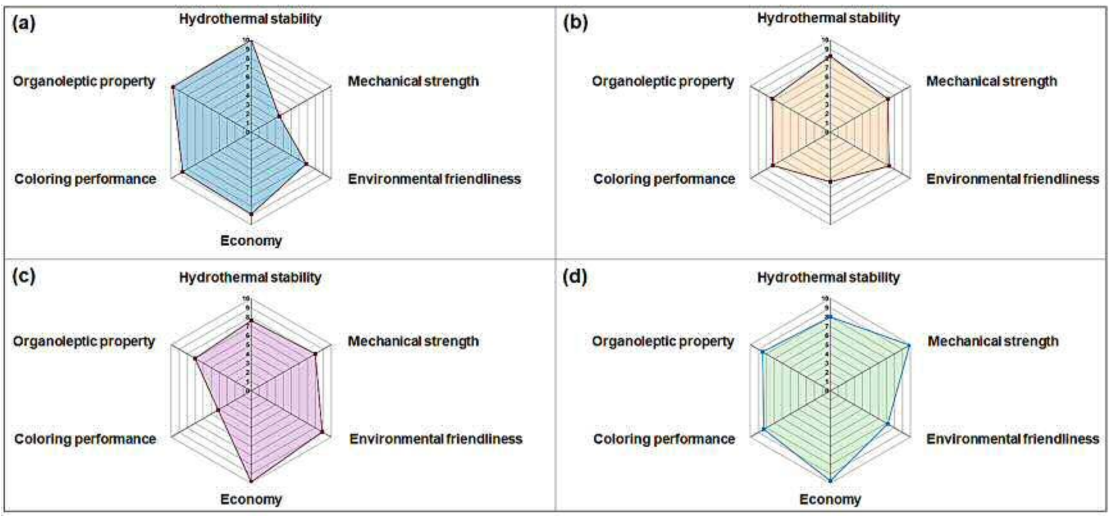

Fig. 7. Comprehensive performance comparison of the crust leathers from different processing strategies: (a) Cr; (b) HAZ; (c) BAT; (d) BAT-TAT.

4. Conclusions

In our pioneering BAT-TAT strategy, a biomass-based aldehyde (BAT) tanning agent has been efficiently utilized via the incorporation into the process of a subsequent terminal aluminum tanning treatment (TAT). FTIR, XPS and TG-DSC analyses showed that the introduction of the TAT could provide additional crosslinks to construct a more robust interlocking network among the post-tanning materials, the residues of the BAT and the carboxyl groups of the collagen fibers. After the TAT, most post-tanning materials could be fixed in the BAT-TAT leather crust efficiently. On account of this, the physical properties of the resultant BAT leather, in terms of mechanical strength, organoleptic properties and coloring performance, were substantially improved. Such improvements took place to a level that the resultant BAT-TAT leather showed comparable physical properties to the crust leather prepared using a conventional chrome tanning methodology, not to mention the additional advantages, in terms of environmental friendliness and economy, of our novel methodology. As such, this BAT-TAT strategy can overcome the existing drawbacks of the BAT tanning system, showing favorable prospects for commercial applications. These findings are a step-change in the race for developing cleaner integrated technology systems to produce high-performance chrome-free leather, aiming to ensure the viable and sustainable development of the leather industry.

Acknowledgments

This work was financially supported by the National Key R&D Program [grant number 2020YFE0203800] and the National Natural Science Foundation of China [grant numbers 22108297, 52073301]. Javier Remón is grateful to the Spanish Ministry of Science, Innovation and Universities for the Juan de la Cierva (JdC) fellowship [grant number IJC2018-037110-I]. The authors thank Dr. Xiu He at the College of Biomass Science and Engineering, Sichuan University, for her experimental assistance.

References

Anjali, T., 2012. Modification of carboxymethyl cellulose through oxidation. Carbohydr. Polym. 87, 457–460. https://doi.org/10.1016/j.carbpol.2011.08.005

Bai, X., Chang, J., Chen, Y., Fan, H., Shi, B., 2013. A Novel Chromium-free Tanning Process Based on In-situ Melamine-formaldehyde Oligomer Condensate. J. Am. Leather Chem. Assoc. 108, 404–410.

Cohen, N.S., Odlyha, M., Foster, G.M., 2000. Measurement of shrinkage behaviour in leather and parchment by dynamic mechanical thermal analysis. Thermochim. Acta 365, 111–117. https://doi.org/10.1016/S0040-6031(00)00618-3

Covington, A.D., 2009. Tanning chemistry: the science of leather. Royal Society of Chemistry, Cambridge.

Ding, W., Cheng, Y., Wang, Y., Shi, B., 2015. Chrome-reduced combination tanning for cleaner dyed sheep fur processing. J. Am. Leather Chem. Assoc. 110, 363–371.

Ding, W., Guo, S., Liu, H., Pang, X., Ding, Z., 2021. Synthesis of an amino-terminated waterborne polyurethane-based polymeric dye for high-performance dyeing of biomass-derived aldehyde-tanned chrome-free leather. Mater. Today Chem. 21, 100508. https://doi.org/10.1016/j.mtchem.2021.100508

Ding, W., Pang, X., Ding, Z., Tsang, D.C.W., Jiang, Z., Shi, B., 2020. Constructing a robust chrome-free leather tanned by biomass-derived polyaldehyde via crosslinking with chitosan derivatives. J. Hazard. Mater. 396, Article 122771.

Ding, W., Wang, Y., Zhou, J., Shi, B., 2018a. Effect of structure features of polysaccharides on properties of dialdehyde polysaccharide tanning agent. Carbohydr. Polym. 201, 549–556. https://doi.org/10.1016/j.carbpol.2018.08.111

Ding, W., Wu, Y., 2020. Sustainable dialdehyde polysaccharides as versatile building blocks for fabricating functional materials: An overview. Carbohydr. Polym. 248, 116801. https://doi.org/10.1016/j.carbpol.2020.116801

Ding, W., Yi, Y., Wang, Y., Zhou, J., Shi, B., 2019. Peroxide-periodate co-modification of carboxymethylcellulose to prepare polysaccharide-based tanning agent with high solid content. Carbohydr. Polym. 224, Article 115169. https://doi.org/10.1016/j.carbpol.2019.115169

Ding, W., Yi, Y., Wang, Y., Zhou, J., Shi, B., 2018b. Preparation of a highly effective organic tanning agent with wide molecular weight distribution from bio-renewable sodium alginate. ChemistrySelect 3, 12330–12335. https://doi.org/10.1002/slct.201802540

Ding, W., Zhou, J., Zeng, Y., Wang, Y., Shi, B., 2017. Preparation of oxidized sodium alginate with different molecular weights and its application for crosslinking collagen fiber. Carbohydr. Polym. 157, 1650–1656. https://doi.org/10.1016/j.carbpol.2016.11.045

Gao, D., Cheng, Y., Wang, P., Li, F., Wu, Y., Lyu, B., Ma, J., Qin, J., 2020. An eco-friendly approach for leather manufacture based on P(POSS-MAA)-aluminum tanning agent combination tannage. J. Clean. Prod. 257, Article 120546. https://doi.org/10.1016/j.jclepro.2020.120546

Hao, D., Wang, X., Liu, X., Zhu, X., Sun, S., Li, J., Yue, O., 2020. A novel eco-friendly imidazole ionic liquids based amphoteric polymers for high performance fatliquoring in chromium-free tanned leather production. J. Hazard. Mater. 399. https://doi.org/10.1016/j.jhazmat.2020.123048

He, X., Ding, W., Yu, Y., Zhou, J., Shi, B., 2020. Insight into the Correlations Between Fiber Dispersion and Physical Properties of Chrome Tanned Leather. J. Am. Leather Chem. Assoc. 115, 23–29.

He, X., Huang, Y., Xiao, H., Xu, X., Wang, Y., Huang, X., Shi, B., 2021. Tanning agent free leather making enabled by the dispersity of collagen fibers combined with superhydrophobic coating. Green Chem. 23, 3581–3587. https://doi.org/10.1039/d1gc00380a

He, X., Wang, Y., Zhou, J., Wang, H., Ding, W., Shi, B., 2019. Suitability of Pore Measurement Methods for Characterizing the Hierarchical Pore Structure of Leather. J. Am. Leather

Chem. Assoc. 114, 41–47.

Hedberg, Y.S., 2020. Chromium and leather: a review on the chemistry of relevance for allergic contact dermatitis to chromium. J. Leather Sci. Eng. 2, 20. https://doi.org/10.1186/s42825-020-00027-y

ISO 11640:2012, n.d. Leather-Tests for colour fastness-Colour fastness to cycles of to-and-fro rubbing.

ISO 2420:2017, n.d. Leather-Physical and mechanical tests-Determination of apparent density and mass per unit area.

IUP 36, 2000. Measurement of leather softness. J. Soc. Leath. Tech. Ch 84, 377–379.

IUP 6, 2000. Measurement of tensile strength and percentage elongation. J Soc Leather Technol Chem 84, 317–321.

IUP 8, 2000. Measurement of tear load-double edge tear. J. Soc. Leather Technol. Chem 84, 327–329.

Jia, X., Tan, R., Peng, B., 2021. Preparation and application of polyethylene glycol triazine derivatives as a chrome-free tanning agent for wet-white leather manufacturing. Environ. Sci. Pollut. Res. 1–11. https://doi.org/10.1007/s11356-021-16133-1

Jia, X., Zhang, C., Ali Chattha, S., Peng, B., 2020. A salt-free pickling chrome tanning technology: Pretreatment with the collective polyoxyethylene diepoxy ether and urotropine. J. Clean. Prod. 244, 1–8. https://doi.org/10.1016/j.jclepro.2019.118706

Jiang, Z., Gao, M., Ding, W., Huang, C., Hu, C., Shi, B., Tsang, D.C.W., 2021. Selective degradation and oxidation of hemicellulose in corncob to oligosaccharides: From biomass into masking agent for sustainable leather tanning. J. Hazard. Mater. 413, 125425.

https://doi.org/10.1016/j.jhazmat.2021.125425

Jones, M., Gandia, A., John, S., Bismarck, A., 2021. Leather-like material biofabrication using fungi. Nat. Sustain. 4, 9–16. https://doi.org/10.1038/s41893-020-00606-1

Joseph, K., Nithya, N., 2009. Material flows in the life cycle of leather. J. Clean. Prod. 17, 676–682. https://doi.org/10.1016/j.jclepro.2008.11.018

Korpe, S., Bethi, B., Sonawane, S.H., Jayakumar, K. V, 2019. Tannery wastewater treatment by cavitation combined with advanced oxidation process (AOP). Ultrason. Sonochem. 59, 104723.

Krishnamoorthy, G., Sadulla, S., Sehgal, P.K., Mandal, A.B., 2013. Greener approach to leather tanning process: D-Lysine aldehyde as novel tanning agent for chrome-free tanning. J. Clean. Prod. 42, 277–286. https://doi.org/10.1016/j.jclepro.2012.11.004

Li, J., Yan, L., Shi, B., Li, B., Zhang, J., 2013. A Novel Approach to Clean Tanning Technology. J. Chem. Chem. Eng. 7, 1203–1212.

Liu, J., Luo, L., Hu, Y., Wang, F., Zheng, X., Tang, K., 2019. Kinetics and mechanism of thermal degradation of vegetable-tanned leather fiber. J. Leather Sci. Eng. 1, 9. https://doi.org/10.1186/s42825-019-0010-z

Liu, X., Wang, W., Wang, X., Sun, S., Wei, C., 2021. A " Taiji-Bagua " inspired multi-functional amphoteric polymer for ecological chromium-free organic tanned leather production : Integration of retanning and fatliquoring. J. Clean. Prod. 319, 128658.

Ma, J., Yang, N., Li, Y., Gao, D., Lyu, B., Zhang, J., 2021. A cleaner approach to tanning process of cattle hide upper suede leather: chrome-less polycarboxylate/montmorillonite nanocomposites as tanning agent. Environ. Sci. Pollut. Res. 1–12.

Ma, J., Yang, Z., Lu, S., Cheng, X., Wang, W., Feng, L., Hu, G., 2002. The correlation between the comonomer ratios of vinyl polymer tannages and their application properties. J. Soc. Leather Technol. Chem. 86, 47–54.

Meng, W., Khayat, K., 2017. Effects of saturated lightweight sand content on key characteristics of ultra-high-performance concrete. Cem. Concr. Res. 101, 46–54. https://doi.org/10.1016/j.cemconres.2017.08.018

Meng, W., Valipour, M., Khayat, K.H., 2017. Optimization and performance of cost-effective ultra-high performance concrete. Mater. Struct. Constr. 50, 1–16. https://doi.org/10.1617/s11527-016-0896-3

Pang, X., Ding, Z., Ding, W., Xiao, X., Liao, X., Shi, B., 2019. Investigation of the Synthesis of a Novel Glycidyl Ether-amine Epoxy Tanning Agents and their Tanning Performance. J. Am. Leather Chem. Assoc. 114, 228–239.

Peng, W., Zhang, X., Chen, S., 2006. The principle and method of testing leather fullness and softness. J. Soc. Leather Technol. Chem. 90, 117–122.

Selvaraj, R., Santhanam, M., Selvamani, V., Sundaramoorthy, S., Sundaram, M., 2018. A membrane electroflotation process for recovery of recyclable chromium (III) from tannery spent liquor effluent. J. Hazard. Mater. 346, 133–139.

Sivagami, K., Sakthivel, K.P., Nambi, I.M., 2018. Advanced oxidation processes for the treatment of tannery wastewater. J. Environ. Chem. Eng. 6, 3656–3663.

Sreeram, K.J., Rao, J.R., Chandrababu, N.K., Nair, B.U., Ramasami, T., 2006. High exhaust chrome-aluminium combination tanning: Part 1. Optimization of tanning. J. Am. Leather Chem. Assoc. 101, 86–95.

Tang, Y., Zhao, J., Zhou, J., Zeng, Y., Zhang, W., Shi, B., 2020. Highly efficient removal of Cr (III)-poly (acrylic acid) complex by coprecipitation with polyvalent metal ions: Performance, mechanism, and validation. Water Res. 178, 115807.

Wang, X., Sun, S., Zhu, X., Guo, P., Liu, X., Liu, C., Lei, M., 2021a. Application of amphoteric polymers in the process of leather post-tanning. J. Leather Sci. Eng. 3, 1–9.

Wang, X., Wang, W., Liu, X., Wang, Y., 2021b. Amphoteric functional polymers for leather wet finishing auxiliaries: A review. Polym. Adv. Technol. 32, 1951–1964. https://doi.org/10.1002/pat.5248

Wang, Y., Shi, B., 2019. Progress of inverse chrome tanning technology. Chem. Ind. Eng. Prog. 38, 639–648.

Wang, Y., Sun, X., Han, Q., James, T.D., Wang, X., 2021. Highly sensitive and selective water-soluble fluorescent probe for the detection of formaldehyde in leather products. Dye. Pigment. 188, 109175. https://doi.org/10.1016/j.dyepig.2021.109175

Wang, Z., Yao, M., Wang, X., Li, S., Liu, Y., Yang, G., 2020. Influence of reaction media on synthesis of dialdehyde cellulose/GO composites and their adsorption performances on heavy metals. Carbohydr. Polym. 232, Article 115781. https://doi.org/10.1016/j.carbpol.2019.115781

Xu, T., Jiang, X., Tang, Y., Zeng, Y., Zhang, W., Shi, B., 2021. Oxidation of trivalent chromium induced by unsaturated oils: A pathway for hexavalent chromium formation in soil. J. Hazard. Mater. 405, 124699. https://doi.org/10.1016/j.jhazmat.2020.124699

Yi, Y., Jiang, Z., Yang, S., Ding, W., Wang, Y., Shi, B., 2020. Formaldehyde formation during the preparation of dialdehyde carboxymethyl cellulose tanning agent. Carbohydr. Polym.

239, Article 116217.

Yu, Y., Lin, Y., Zeng, Y., Wang, Y., Zhang, W., Zhou, J., Shi, B., 2021. Life Cycle Assessment for Chrome Tanning, Chrome-Free Metal Tanning, and Metal-Free Tanning Systems. ACS Sustain. Chem. Eng. https://doi.org/10.1021/acssuschemeng.1c00753

Yu, Y., Wang, Y. nan, Ding, W., Zhou, J., Shi, B., 2017. Preparation of highly-oxidized starch using hydrogen peroxide and its application as a novel ligand for zirconium tanning of leather. Carbohydr. Polym. 174, 823–829. https://doi.org/10.1016/j.carbpol.2017.06.114

Yu, Y., Zeng, Y., Wang, Y., Liang, T., Zhou, J., Shi, B., 2020. Inverse chrome tanning technology: a practical approach to minimizing Cr(III) discharge. J. Am. Leather Chem. Assoc. 115, 176–183.